



Monomethyl Auristatin E (MMAE), a Payload for Multiple Antibody Drug Conjugates (ADCs), Demonstrates Differential Red Blood Cell Partitioning Across Human and Animal Species

Victor Yip, Ola M. Saad, Doug Leipold, Chunze Li, Amrita Kamath & Ben-Quan Shen

To cite this article: Victor Yip, Ola M. Saad, Doug Leipold, Chunze Li, Amrita Kamath & Ben-Quan Shen (22 Apr 2024): Monomethyl Auristatin E (MMAE), a Payload for Multiple Antibody Drug Conjugates (ADCs), Demonstrates Differential Red Blood Cell Partitioning Across Human and Animal Species, Xenobiotica, DOI: [10.1080/00498254.2024.2345849](https://doi.org/10.1080/00498254.2024.2345849)

To link to this article: <https://doi.org/10.1080/00498254.2024.2345849>



© 2024 The Author(s). Published by Informa UK Limited, trading as Taylor & Francis Group



Accepted author version posted online: 22 Apr 2024.



[Submit your article to this journal](#)



Article views: 569



[View related articles](#)



[View Crossmark data](#)

Running Title: MMAE RBC Partitioning in Human and Animal Bloods
Monomethyl Auristatin E (MMAE), a Payload for Multiple Antibody Drug
Conjugates (ADCs), Demonstrates Differential Red Blood Cell Partitioning
Across Human and Animal Species

Victor Yip^a, Ola M. Saad^b, Doug Leipold^a, Chunze Li^c, Amrita Kamath^a and Ben-Quan Shen^{a,*}

^aPreclinical and Translational Pharmacokinetics and Pharmacodynamics, Genentech Inc., 1 DNA Way, South San Francisco, CA 94080

^bBioAnalytical Sciences, Genentech Inc., 1 DNA Way, South San Francisco, CA 94080

^cClinical Pharmacology, Genentech Inc., 1 DNA Way, South San Francisco, CA 94080

***Corresponding author:** Ben-Quan Shen, M.D. Preclinical and Translational Pharmacokinetics and Pharmacodynamics, Genentech Inc. 1 DNA Way, South San Francisco, CA 94080. Email: bqshen@gene.com; shen.ben@gene.com

Abstract

- 1. Background:** Monomethyl auristatin E (MMAE) has been used as a payload for several Food and Drug Administration (FDA) approved antibody-drug conjugates (ADCs). It is known that MMAE is released from the ADC following binding, internalization and proteolytic degradation in target tissues. A striking discrepancy in systemic MMAE levels has been observed across species with 50-fold higher MMAE levels in human than that in rodents when normalized by ADC dose with unknown mechanism.
- 2. Hypothesis and purpose:** Multiple factors could affect systemic MMAE levels such as production and elimination of unconjugated MMAE following ADC dosing. In this

study, we have explored whether MMAE displays differential red blood cell (RBC) partitioning across species that may contribute to the different MMAE levels seen between human and animals.

- 3. Experiments:** To determine MMAE RBC partitioning, tritium labeled MMAE ($[^3\text{H}]$ -MMAE) was incubated in whole blood from mice, rats, monkeys and humans *in vitro*, then RBC partitioning was determined and compared across species. To test whether MMAE released from the ADC would show any difference in RBC partitioning, pinatuzumab vedotin or polatuzumab vedotin was administered to mice, rats, and monkeys. MMAE levels were measured in both blood and plasma, and the ratios of MMAE levels were calculated as blood-to-plasma ratio (*in vivo* RBC partitioning).
- 4. Results:** Our *in vitro* data showed that unconjugated MMAE has a species-dependent RBC partitioning with strong RBC partitioning in mouse, rat, followed by monkey blood, whereas minimal RBC partitioning was seen in human blood. Incubation of 2 nM of MMAE in mouse blood resulted in a blood-to-plasma ratio of 11.8 ± 0.291 , followed by rat, monkey, and human at 2.36 ± 0.0825 , 1.57 ± 0.0250 , and 0.976 ± 0.0620 , respectively. MMAE RBC partitioning is also concentration-dependent, with an inverse relationship between RBC partitioning and MMAE concentration (higher RBC partitioning at lower concentration). *In vivo* dosing of pinatuzumab vedotin in mouse displayed systemic MMAE at about a 5-fold higher blood concentration compared to plasma concentration once MMAE reached a pseudo-equilibrium, while systemic MMAE from blood and plasma concentration showed a 1.65-fold difference in rat.
- 5. Implication and conclusion:** These data demonstrated that MMAE has a distinct RBC partitioning across different species, which may contribute to, at least in part, to the

differential in the systemic MMAE levels observed *in vivo* between preclinical and clinical studies. These findings highlight the importance of fully characterizing the ADME properties of both the ADC and its payload, to enable better translation from animals to human for ADC development.

Keyword: Monomethyl auristatin E, antibody-drug conjugate, blood partition, polatuzumab vedotin

Introduction

Antibody-drug conjugates (ADCs) are a therapeutic class that utilizes a highly potent cytotoxic payloads having narrow therapeutic window if administered alone. However, with conjugation of the payloads to a monoclonal antibody via a linker, the ADC would allow the specific delivery of payload to tumor target by using the antibody's specificity, as such reducing systemic exposure and normal tissues uptake, thus, increasing the therapeutic window (Lucas et al., 2018; Junutula et al., 2008). Auristatins are important payloads used in ADCs, and monomethyl auristatin E (MMAE) is the most well-known compound in the family having been used in four Food and Drug Administration (FDA)-approved ADCs (Brentuximab vedotin, Polatuzumab vedotin, Enfortumab vedotin, and Tisotumab vedotin) (Akaiwa et al., 2020).

MMAE is a very potent antimetabolic agent that inhibits cell division by blocking the polymerization of tubulin and it is 100 times more potent than doxorubicin, a chemotherapy medication (Gualberto, 2012). As such, targeted therapeutic options such as conjugation on to

an ADC, is needed to deliver MMAE to cancer cells while sparing normal cells. MMAE is known to be released due to deconjugation by cathepsin B cleavage and/or catabolism of ADCs after internalization into cells, and detected systemically (Gikanga et al., 2016; Caculitan et al., 2017). As a result, adverse effects (AEs) such as hematological toxicity and peripheral neuropathy has been observed in patients who received MMAE-containing ADCs in the clinic (Donaghy, 2016; Masters et al., 2018). Exposure response analyses showed a positive correlation of circulating unconjugated MMAE exposure with some of hematological adverse effects (e.g., Grade 3 Anemia) (Lu et al., 2020), while other AEs (e.g., peripheral neuropathy) were correlated well with antibody-conjugated MMAE levels, suggesting that these toxicity events are likely due to the release of MMAE following the distribution of ADC to non-targeted tissue (Lu et al., 2015, Li et al., 2020).

Interestingly, there were minimally detectable levels of unconjugated MMAE in plasma following dosing ADC at 5 mg/kg in mice and rats in our PK studies. Similar observation was made by Zhang et al. (2021) who used a different targeting MMAE-containing ADC. In contrast, strikingly higher MMAE levels were observed in human plasma following ADC dosing in comparison to that seen in monkey and rodent when normalized by ADC dose (**Table 1**). Currently, it is unknown what causes the lack of direct correlation in MMAE levels following ADC dosing between humans and animals, which makes it difficult to translate from the preclinical data to human (Li et al., 2020).

MMAE, like many other small molecules tested clinically, has been studied by *in vitro* assays and limited *in vivo* studies since it cannot be administered safely as an unconjugated small molecule except at very low doses. Previously, it was reported that MMAE partitions to erythrocytes (red blood cells, RBCs) with a blood-to-plasma ratio of about 6 when unconjugated

MMAE is administered to xenograft bearing mice (Chang et al., 2021). However, to this date there is no data providing a direct comparison of MMAE RBC partitioning across species. Like the plasma protein binding for small molecules, RBC partitioning can also impact the amount of drugs available for the targets as well as the distribution and elimination rate of the drugs. Furthermore, it often acts as a depot to sequester the drug if such binding is reversible (Kwakye et al., 2018).

In this manuscript, we have tested whether MMAE has any differential RBC partitioning across different species using both *in vitro* and *in vivo* approaches, which may contribute to the different unconjugated MMAE levels observed across CD1/SCID mice, Sprague Dawley (SD) rats, cynomolgus monkeys and humans following ADC dosing. Our results demonstrated a species- and concentration-dependent of MMAE RBC partitioning, which may serve as the first step to dissect the observed unconjugated MMAE level discrepancy from preclinical species to human, and also highlights the importance of understanding the ADME properties for both ADCs and their highly potent cytotoxic payloads.

Materials and Methods

MMAE, Pinatuzumab Vedotin and Polatuzumab Vedotin

All unconjugated antibodies used for *in vivo* studies presented here were generated at Genentech Inc. (South San Francisco, CA). The unconjugated mAb, pinatuzumab, is a humanized monoclonal IgG1 antibody that binds to the CD22 human receptor and does not cross-react with rodent CD22. Polatuzumab is a humanized monoclonal IgG1 antibody that binds to the CD79b

human receptor and does not cross-react with rodent CD79b. The payload, MMAE, was obtained from Seagen Inc.(Bothell, WA). The conjugation of mAb and payload to form pinatuzumab vedotin and polatuzumab vedotin was performed as described previously (Doronina et al., 2003). Briefly, polatuzumab vedotin was prepared by incubating the maleimide drug derivative with the partially reduced antibodies for 1 hour at 4°C. After quenching the reaction with excess *N*-acetylcysteine to react with any free linker–drug, the conjugated antibody was purified. Conjugation conditions were chosen to achieve an average drug-to-antibody ratio (DAR) of approximately 3.4-3.5. ADC protein concentrations were calculated using absorbance at 280 nm (320-nm reference) and the molar extinction coefficient of the antibody. The average DARs were calculated from the integrated areas of the DAR species resolved by hydrophobic interaction chromatography on an analytical column (TSK butyl-NPR 4.6 mm, 10 cm, and 2.5 mm, Tosoh Bioscience, South San Francisco, CA).

Radiochemistry

[³H]-MMAE was obtained from Seagen Inc. (Bothell, WA) with a specific activity of 33.8 μCi/μg. [³H]-MMAE with a maleimidocaproyl-valine-citrulline-p-aminobenzyloxycarbonyl (MC-vc-PAB) linker with a specific activity of 19.9 μCi/μg (Seagen Inc., Bothell, WA) was conjugated to mAb as described in the above “MMAE, pinatuzumab vedotin, and polatuzumab vedotin” section. The resulting [³H]-MMAE ADC had a specific activity of 29.3 μCi/mg and a DAR of 3.4. The structure of the linker, drug, and the radiolabeled ³H location is shown in **Figure 1**.

***In vitro* assessment of MMAE blood partitioning**

To assess the potential of MMAE partitioning to the RBC in whole blood *in vitro* across human and preclinical species, [³H]-MMAE at 0.25 uCi was mixed with unlabeled MMAE to a final concentration ranging from 2 nM to 5,000 nM and incubated in human, cynomolgus monkey, Sprague Dawley (SD) rat and CD1 mouse blood. Human and animal blood with lithium heparin were purchase from BioIVT (Westbury, NY). All blood samples have a hematocrit between 38% to 45%. After 60 minutes of incubation at 37°C and 5% CO₂ (enough time to reach equilibrium), the blood samples were collected and further processed to plasma and cell pellet fraction. [³H]-Chloroquine (MT-1885, Moravek Biochemical, Brea, CA) and [³H]-Verapamil (NET810025UC, Perkin Elmer, Boston, MA) were used as known published high and low RBC partitioning control (Yu et al., 2005) in this study as the same assessment as MMAE.

Blood (plasma and cell pellet) samples were processed for liquid scintillation counting described previously in Shen et al. (Shen et al., 2012). Briefly, whole blood was separated by centrifugation at 3,500 relative centrifugal force (RCF) for 5 minutes at 4°C to generate a plasma fraction and a cell pellet fraction, which included both RBC and peripheral blood mononuclear cell (PMBC). Each plasma or cell pellet sample was first solubilized by mixing with SOLVABLE™ (No. 6NE9100, PerkinElmer; Shelton, CT). Then, the sample coloration was quenched using 30% H₂O₂ and the quenched samples were mixed with Ultima Gold™ MV Liquid Scintillation Cocktail (No. 6013159, PerkinElmer). The total radioactivity of the processed samples was measured using a Tri Carb™ 2900TR liquid scintillation analyzer (LSC) (PerkinElmer, Billerica, MA). The result radioactivity count in whole blood and plasma was calculated as blood and plasma concentration based on hematocrit to determine the blood-to-plasma ratio and the potential of MMAE RBC partitioning.

In addition, we also conducted an experiment to understand whether the MMAE interaction with RBCs was reversible. Once again, 2 nM of [³H]-MMAE/unlabeled MMAE was incubated in mouse blood at 37°C with 5% CO₂ for 30 minutes. After incubation, the blood samples were processed for plasma and cell pellet where the plasma was removed and replaced with fresh plasma. The sample was then further incubated at 37°C with 5% CO₂ for an additional 30, 60, and 120 minutes. The blood samples were once again processed for plasma and cell pellet, then analyzed using the LSC to determine radioactivity level to obtain blood-to-plasma ratio of the samples.

Further investigation was warranted to understand the mechanism of the observed MMAE RBC partitioning in rodents, particularly in mouse. An experiment was to determine if the MMAE was partitioning to the cell pellet by RBC or by PBMC. 2 nM of [³H]-MMAE/unlabeled MMAE mixture was added to mouse blood and was incubated at 37°C with 5% CO₂ for 30 minutes. Then the blood was either separated to plasma and cell pellet (RBC + PBMC) by centrifugation or mixed with FICOLL 400* (Sigma-Aldrich cat# F4375, St. Louis, MO) to create a Ficoll gradient for separation of plasma with PBMC and RBC. Each fraction was collected and was analyzed by using the LSC to determine radioactivity level.

***In vivo* assessment of MMAE red blood cell partitioning**

To understand the *in vivo* MMAE blood partitioning to RBC, fifteen female SD rats with jugular-vein cannulation each weighing about 200 g were obtained from Charles River Laboratories (Reno, NV). The rats were given an intravenous (IV) bolus dose of [³H]-MMAE mixed with unlabeled MMAE at 200 µg/kg (~80 µCi/kg radioactivity level). Blood samples (~0.3 mL) were collected from the jugular cannula at multiple time points post IV administration. To obtain

plasma, blood was collected into lithium heparin tubes and gently inverted several times to properly mix the anticoagulant (lithium-heparin) at several time points up to 6 hours. Blood (plasma and cell pellet) samples were processed for liquid scintillation counting. The result radioactivity count in plasma and blood (the summation of plasma and cell pellet fraction) was calculated as blood and plasma concentration to determine the blood-to-plasma ratio and the MMAE RBC partitioning. All the protocols and procedures for animal studies in this paper were reviewed and approved by the Genentech Institutional Animal Care and Use Committee (IACUC) and performed in accordance with the institutional and regulatory guidelines.

***In vivo* assessment of unconjugated MMAE blood partitioning from pinatuzumab/polatuzumab vedotin**

Twenty female SCID mice weighing about 20 to 25 g were obtained from Charles River Laboratories (Hollister, CA). Pinatuzumab vedotin was administered intravenously at 5 mg/kg via tail vein injection. At selected time point from 5 minutes to 14 days post-dose, 150 μ L of blood was collected through the retro-orbital. 60 μ L of the blood was transferred into a separate tube containing 240 μ L sterile water and the other 90 μ L for blood was processed for plasma by centrifugation at 12,800 RCF for 5 minutes at 4°C. The samples then underwent protein precipitation with a 4:1 acetonitrile with MMAE-d8 to sample (v/v) to obtain the soluble fraction. Supernatants were analyzed by LC-MS/MS. Samples were analyzed by Turnolon Spray using an API 3000 mass spectrometer (Applied Biosystems; Foster City, CA) updated with an HSID interface (Ionics Mass Spectrometry Group, Inc.; Ontario, Canada). The HPLC system used for analysis was a Shimadzu HPLC LC-10ADvp system (Shimadzu Scientific Instruments; Columbia, MD), equipped with a short Hot Pocket column heater (Keystone Scientific, Inc.; Bellefonte, PA) and analytical column (Phenomenex Synergi MAX-RP 80A,

C12, 4 μ m, 2.0 \times 50 mm) at 25°C. The multiple-reaction monitoring scan mode was used for quantitation. For MMAE quantitation, transition 726.6/152.1 was monitored for MMAE-d8 (internal standard), and transition 718.7/152.2 was monitored for MMAE. The LC-MS/MS assay had an LLOQ of 0.0352 ng/mL (0.0490 nM) with linearity demonstrable up to 18.0 ng/mL (25.0 nM) upper limit of quantitation using a sample volume of 0.015 mL. The measured MMAE concentrations were plotted as time-vs.-concentration graph.

Similarly, five female SD rats (weighing about 300 g each obtained from Charles River Laboratories (Reno, NV)) also dosed intravenously at 5 mg/kg of Pinatuzumab vedotin via tail vein injection with various blood collections time points from 5 minutes to 14 days post-dose. 200 μ L of blood was collected through the tail vein which half was separated into a tube containing 400 μ L of sterile water and the other half was processed for plasma by centrifugation at 12,800 RCF for 5 minutes at 4°C. The samples then underwent protein precipitation with a 4:1 acetonitrile with MMAE-d8 to sample (v/v) to obtain the soluble fraction. Supernatants were analyzed by LC-MS/MS and the measured concentrations were plotted as time-vs.-concentration graph. Blood and plasma concentration was used to determine the blood-to-plasma ratio.

Finally, three male cynomolgus monkeys (weighting 3 to 4 kg each from Charles River Laboratories (Reno, NV)) were dosed intravenously at 1mg/kg of polatuzumab vedotin via the saphenous vein with various blood collection time points from 15 minutes to 22 days post-dose. 1.5 mL of blood was collected in which 25 μ L of blood was separated into a tube containing 100 μ L of sterile water. The remaining blood was processed for plasma by centrifugation at 1,500 to 2,000 RCF for 10-15 minutes. The samples then underwent protein precipitation with a 4:1 acetonitrile with MMAE-d8 to sample (v/v) to obtain the soluble fraction. Supernatants were

analyzed by LC-MS/MS and the measured concentrations were plotted as time-vs.-concentration graph. Blood and plasma concentration was used to determine the blood-to-plasma ratio.

Data Analysis

Each blood and plasma paired sample was analyzed with a resulted concentration in ng/mL or %ID/mL, then a blood-to-plasma ratio is calculated by dividing the blood concentration to the plasma concentration. As the blood-to-plasma ratio increases, the higher the RBC partitioning is. All samples where hematocrit was not analyzed, the default hematocrit used was 40% with the understanding of hematocrit can varies between species (Davies and Morris, 1993). *In vivo* PK analysis was done using Phoenix WinNonlin (Pharsight, St. Louis, MO) using a non-compartment model and PK parameters such as maximum concentration (C_{max}), Area-under-the-curve (AUC, using the trapezoidal rule from the timepoints indicated), and dose normalized concentration are calculated.

Results

MMAE RBC partitioning is different across species following incubation of unconjugated MMAE in whole blood from rodents, monkeys and humans

The blood-to-plasma ratio for [3 H]-MMAE showed concentration-dependent RBC partitioning in animal blood; at lower concentrations of 2, 20, and 200 nM, the blood-to-plasma ratios were greater than 1, but at higher concentrations of 1,000 and 5,000 nM, the blood-to-plasma ratio were less than 1 (**Figure 2A**). There was also a species dependent RBC partitioning trend in which mouse had the highest partitioning, followed by rat and cynomolgus monkey. In mouse

blood, the highest observed RBC partitioning was at 2 nM where blood-to-plasma ratio was 11.8. The partitioning in animal blood was saturable at concentration higher than 1000nM. Molecule with blood-to-plasma ratio of greater than 1 is considered to be strongly associated with RBCs. The blood-to-plasma ratio of MMAE in human blood was at or less than 1 in the concentrations tested, which suggested that MMAE had minimal RBC partitioning in human blood.

Chloroquine is known to have high RBC partitioning (Yu et al., 2005) and has a blood-to-plasma ratio of greater than 1. In this study, the *in vitro* blood-to-plasma ratio for [³H]-chloroquine was greater than 1 in all tested species and at all concentrations (**Figure 2B**). Meanwhile, verapamil is known to have low RBC partitioning (Yu et al., 2005) as indicated by blood-to-plasma ratio of less than 1. In this study, the blood-to-plasma ratio for [³H]-verapamil was less than 1 in all tested species and at all concentrations (**Figure 2C**).

MMAE RBC Partitioning is Reversible in Mice

To elucidate whether the MMAE partitioning to cell pellet was whether associated with RBC and/or PBMC, a Ficoll separation method was performed after [³H]-MMAE was incubated with mouse blood. After incubation, the samples that were separated for plasma and cell pellet showed similar results as previous *in vitro* experiments where blood-to-plasma in mouse blood was 6.75 while in human blood was 0.98. In mouse blood, the plasma consisted of 8.9% of the radioactivity while the cell pellet had 91.1%. In the Ficoll separated set of samples, RBC consisted of 82.4% of the radioactivity and thus, we deduced that the PBMC (the other part of the cell pellet) had 8.7% of the radioactivity. As such, we concluded that MMAE partitioned mainly with RBCs and minimally with PBMCs.

Lastly, we examined the reversibility of the MMAE RBC partitioning in mouse blood. In this pulse-chase experiment, [³H]-MMAE was allowed to partition to mouse RBC in blood. This was followed by the removal of the plasma and replacement with fresh plasma (also from blood). Immediately after mixing with the fresh plasma, we determined the blood-to-plasma ratio was 23.7, a significantly higher value than the 6-11 range observed in previous experiments as MMAE was still associated with the RBCs once replaced with fresh plasma. However, after 30 minutes of incubation with the fresh plasma, MMAE reversibly went back to the plasma compartment to establish a new equilibrium with a blood-to-plasma ratio of 8.67 and remained fairly similar at 60 and 120 minutes of incubation.

MMAE demonstrates RBC partitioning *in vivo* following administration of unconjugated MMAE in rats

In a study where rats were dosed intravenously with [³H]-MMAE mixed with unlabeled MMAE, the MMAE RBC partitioning showed that the blood concentration was 0.902-fold comparing to plasma concentration at 5 minutes post-dose (**Figure 3**). The ratio then increased to 5.13 by 45 minutes post-dose and remain fairly stable until the end of the experiment. The comparison between plasma and blood AUC (from 5 minutes to 6 hours) resulted in 3.28-fold higher in blood AUC_(0-6h) to plasma AUC_(0-6h) (15.8 vs. 4.83 %ID*min/mL, respectively).

MMAE demonstrates RBC partitioning *in vivo* following dosing of pinatuzumab vedotin ADC in rodents

After a single dose of intravenously administered pinatuzumab vedotin in rat, the amount of measured unconjugated MMAE in plasma was 0.045 ng/ml at 1 hour post dose and increased to a maximum detected level of 0.37 ng/mL at 72 hours post dose before declining to below

quantification level by 240 hours (**Figure 4**). Meanwhile, the measured level of unconjugated MMAE in blood was 0.55 ng/mL at 1 hour post dose and remained fairly similar to 72 hours post dose. Since blood was diluted in sterile water prior to protein precipitation, all samples after 72 hours post dose were below the quantification level. Overall, all plasma concentrations were lower than blood concentrations for a given sample with a maximum blood-to-plasma ratio of 12.2 at 1 hour post dose to a minimum of 1.65 at 72 hours post dose (**Table 3**). Blood $AUC_{(1h-72h)}$ compared to plasma $AUC_{(1h-72h)}$ showed a ratio of 1.99 over this quantifiable time range.

For mice, the maximum level of detected unconjugated MMAE in both blood and plasma was immediately after dosing, then decreasing over the course of the study (**Figure 5**). At 1 hour post dose, unconjugated MMAE concentration in the blood was 2.41-fold higher than the plasma concentration. As both blood and plasma concentrations decreased, the blood-to-plasma ratio increased to maximum of 6.40 at 72-hours post-dose (**Table 4**). Overall, the ratio of Blood $AUC_{(1h-72h)}$ compared to plasma $AUC_{(1h-72h)}$ was 4.21.

***In vivo* dosing of polatuzumab vedotin ADC in Cynomolgus monkeys**

After a single dose of intravenous administered polatuzumab vedotin in cynomolgus monkey, all blood and plasma samples have an unconjugated MMAE level that were below the lower limit of quantification (0.03 ng/mL in plasma and 0.18ng/mL in blood). Therefore, no further analysis was performed.

Discussion

ADCs are a therapeutic class that utilizes a highly potent cytotoxic payloads that has a narrow therapeutic window if administered alone. However, by conjugating to a monoclonal antibody

via a linker, the ADC provide specificity allowing targeted delivery to the tumor, reduce systemic exposure and normal tissues uptake, thus, increase the therapeutic window. MMAE, a very potent cytotoxic payload has been utilized in several FDA approved ADC therapeutics (Brentuximab vedotin, Polatuzumab vedotin, Enfortumab vedotin, Tisotumab vedotin), has shown rapid elimination from plasma and extensive distribution to multiple highly perfused tissues as well as blood cells when dosed alone in rats (Yip et al., 2021). Once MMAE is stably conjugated to a monoclonal antibody, it is expected that ADC would retain the MMAE with limited amount of unconjugated MMAE potentially generated similarly across species as a result of ADC deconjugation. However, it was observed that the levels of unconjugated MMAE detected in human plasma was much greater than that in the plasma from preclinical species when dose normalized (**Table 1**). In this study, we examined and compared the MMAE RBC partitioning across human and different animal species to understand the impact of MMAE RBC partitioning on the observed differences in unconjugated MMAE levels between human and animal plasma.

From our *in vitro* assessment of MMAE RBC partitioning across human and animal plasma, we found that MMAE has a species- and a concentration-dependent RBC partitioning. Among the species tested, MMAE demonstrates the highest RBC partitioning in mice, followed by rats, monkey, and human (**Figure 2A**). While there was an almost 12-fold higher MMAE concentration in mouse blood compared to plasma at 2 nM of MMAE, concentrations in human blood and plasma were roughly the same when MMAE was spiked at that same concentration. Furthermore, as we increased the amount of MMAE in mouse blood, the blood concentrations became equal to the plasma concentrations, suggesting that the MMAE RBC partition can be saturable with increasing MMAE concentration. However, the saturable concentration of 200 or

1000 nM used in mouse blood would not be a physiologically relevant as the amount of MMAE released from the ADC is often closer to 2 nM.

To delve further into the mechanism of the MMAE RBC partitioning, we performed a pulse-chase experiment in which we first allowed MMAE to partition to RBC in mouse blood (pulse phase). After removing the remaining MMAE in the plasma, we replaced it with plasma from the blood that has not been exposed to MMAE. After reaching equilibrium (chase phase), MMAE was once again detected in the replaced plasma. The blood-to-plasma ratio increased from 6.75, with original plasma and pellet, compared to 8.67 from the replacement plasma and pellet after new equilibrium. This result was reasonable since the new equilibrium has a lower overall MMAE concentration as we removed the original plasma which contained MMAE and replaced it with plasma that did not contain MMAE. Thus, as the concentration of MMAE decrease, the new equilibrium would have a higher blood-to-plasma ratio as MMAE partitioning was concentration-dependent as discussed earlier. Since the MMAE RBC partitioning was reversible, the RBC act as a depot compartment for MMAE and release back into the plasma when the overall concentration in blood decreases. While the hydrophobic nature of MMAE would increase the chance of MMAE associating with the lipid bilayer of the RBC, the concentration-dependent RBC partitioning suggests that these molecules not only partitioned by passive diffusion or hydrophobic interaction but also by other factors such as protein binding facilitated, ion trapping and/or active transport may be involved (Yu et al., 2005). Finally, the species-dependent MMAE RBC partitioning could be due to the differences in blood characteristics across species. For instance, mouse RBCs have a high expression of GLUT4 transporters, but an absence of GLUT1 transporters; whereas the reverse is true for human RBCs (Montel-Hagen et al., 2008). Additional studies are needed to confirm this hypothesis.

In the *in vivo* rat study when unconjugated [3H]-MMAE was dosed, the blood concentration was 5-fold higher than that of the plasma at the same time point suggesting an *in vitro in vivo* correlation (**Figure 3, Table 2**). As such, the quantified levels of MMAE concentration in rodent plasma in preclinical studies would dramatically underestimate the actual MMAE concentration in the blood. Meanwhile, the MMAE concentrations detected in human plasma in the clinic would be a good representative of the MMAE concentrations in blood because of the low potential of MMAE RBC partitioning in human blood if there is a good *in vitro in vivo* correlation.

In the *in vivo* study where we dosed in mice and rats with a MMAE-containing ADC, pinatuzumab vedotin, we found that the released MMAE from the ADC also partitioned with RBCs, similarly as when we dosed MMAE alone. In mice, there was an initial amount of MMAE released into the blood from the ADC after dosing, probably due to the high levels of cathepsin B enzyme, that decreased over the course of the study. As such, at 1 hour post dose, the blood-to-plasma ratio was the lowest at 2.42, increased over the course of the study, and then leveled off at a blood-to-plasma ratio of about 5 as it reached a pseudo-equilibrium at roughly 72 hours post dose (**Figure 4, Table 3**). On the other hand, unconjugated MMAE in rat plasma dosed with pinatuzumab vedotin was low at early time points, then increased until it reached a maximum at around 24 to 72 hours post dose while the levels of unconjugated MMAE detected in rat blood were fairly similar across the first 72 hours. Thus, the blood-to-plasma ratio at 1-hour post-dose was at 12.2, but decreased to only 1.65 at 72 hours post dose (**Figure 5, Table 4**). Our rodent *in vivo* study showed that the extent of MMAE RBC partitioning was higher in mouse blood compared to rat blood which showed good correlation with the *in vitro* studies.

Given that monkey and human MMAE RBC partitioning levels were lower than that of rodent *in vitro*, we expected that the same trend would be observed *in vivo*. Therefore, MMAE RBC partitioning should be minimal (within 2-fold) and the plasma concentration of unconjugated MMAE detected in monkey and human should be a good representation of the respective blood concentrations. Yet, the monkey blood and plasma MMAE concentrations *in vivo* were below the limit of quantification (<0.03 ng/mL in plasma and <0.18 ng/mL in blood) resulting in a greater than 30-fold difference in the amount of unconjugated MMAE detected in human plasma when dose-normalized. Several factors could affect systemic unconjugated MMAE levels across species. These factors include but may not be limited to: (1) differential generation kinetics of unconjugated MMAE from the ADC due to differences in stability (linker type, conjugation site, etc), uptake, and/or catabolism across species; (2) different intrinsic properties of the unconjugated MMAE such as tissue and blood partitioning or plasma protein binding that affect distribution across species; (3) different metabolism and/or elimination rates of unconjugated MMAE across species (Nair & Jacob, 2016). While the MMAE RBC partitioning in rodents may partially explain why unconjugated MMAE levels were lower than that of human, the magnitude of the differences between the clinical and pre-clinical studies also meant these other factors that we have not elucidated might also contribute to the differences of the observed unconjugated MMAE level between species.

Another point to consider in characterizing MMAE RBC partitioning is that many toxicity studies correlated unconjugated MMAE plasma concentration to observed adverse effects since the payload of the ADC is the driver of both therapy and toxicity. As such, the effects of MMAE RBC partitioning in preclinical species, most notably in mice, might underestimate the MMAE concentration translated to human. Furthermore, since RBCs may act as a depot for MMAE in

mouse blood, adverse effects observed in human may be more pronounced as higher systemic levels of unconjugated MMAE might lead to higher levels of unconjugated MMAE in healthy tissues, making translation from preclinical species to human a much more difficult task. While MMAE level in human is much higher than preclinical species, the MMAE (metabolite from ADC) is less than the 10% drug-related material exposure as highlighted by the Metabolite in Safety Testing (MIST) guideline. Nevertheless, given the high potency of MMAE, toxicity studies with unconjugated MMAE were conducted in nonclinical species, including both rats and Cynomolgus monkeys. Furthermore, we also assessed the exposure-response relationship of unconjugated MMAE in context of clinical safety which showed toxicity events were better correlated with antibody-conjugated MMAE levels rather than unconjugated MMAE levels.

Summary and Conclusion

In summary, we have characterized the RBC partitioning of MMAE *in vitro* and *in vivo* using both MMAE or MMAE-ADC across human and animals, and revealed that MMAE has a striking difference in the RBC partitioning with *in vitro* mouse blood-to-plasma ratio of 11.8 ± 0.291 at 2 nM, followed by rat, monkey, and human at 2.36 ± 0.0825 , 1.57 ± 0.0250 , and 0.976 ± 0.0620 , respectively. This RBC partitioning trend correlates well with *in vivo* dosing of MMAE-ADC where unconjugated MMAE levels were 5-fold higher in mouse blood compared to mouse plasma and about 2-fold in rats. This difference seems reversibly correlated with the systemic unconjugated MMAE levels observed between human and animals following ADC dosing. As such, these data may explain, at least in part, the different systemic MMAE levels observed between preclinical and clinical studies following ADC dosing, and highlight the importance of fully characterizing the ADME properties of both the ADC and its payload, to enable better translation from animals to human for ADC development.

Acknowledgements

The authors would like to thank the *In Vivo* Study Group at Genentech for providing support for all *in vivo* studies and the Bioanalytical Group at Genentech for providing support for analysis of the *in vivo* studies samples.

Data Availability

The authors confirm that the data supporting the findings of this study are available within the article.

Disclaimer

The author(s) reported there is no funding associated with the work featured in this article.

Accepted Manuscript

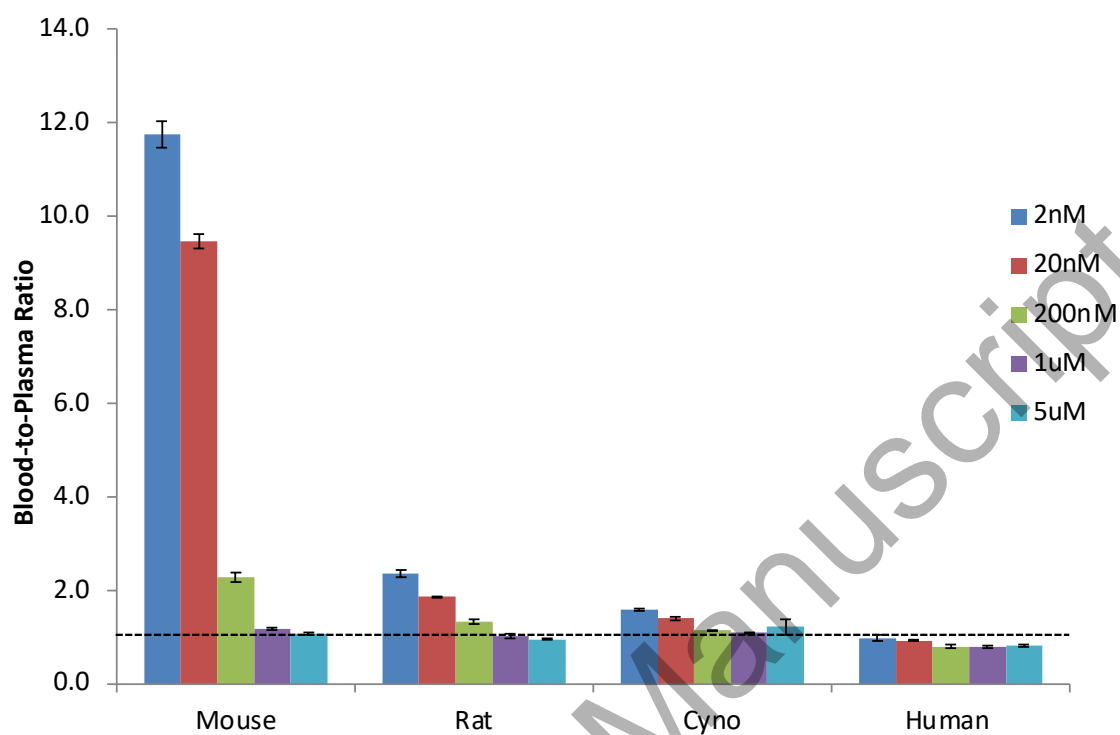
Reference

- Akaiwa M, Dugal-Tessier J, Mendelsohn BA. (2020) Antibody-Drug Conjugate Payloads; Study of Auristatin Derivatives. *Chem Pharm Bull (Tokyo)* **68**:201-211.
- Caculitan NG, Dela Cruz Chuh J, Ma Y, Zhang D, Kozak KR, Liu Y, Pillow TH, Sadowsky J, Cheung TK, Phung Q, et al. (2017) Cathepsin B Is Dispensable for Cellular Processing of Cathepsin B-Cleavable Antibody-Drug Conjugates. *Cancer Res* **77**:7027-7037.
- Chang HP, Cheung YK, Shah DK. (2021) Whole-Body Pharmacokinetics and Physiologically Based Pharmacokinetic Model for Monomethyl Auristatin E (MMAE). *J Clin Med* **10(6)**:1332.
- Davies B, Morris T. (1993) Physiological parameters in laboratory animals and humans. *Pharm Res.* **10(7)**:1093-5.
- Donaghy H. (2016) Effects of antibody, drug and linker on the preclinical and clinical toxicities of antibody-drug conjugates. *MAbs* **8**:659-71.
- Doronina SO, Toki BE, Torgov MY, Mendelsohn BA, Cerveny CG, Chace DF, DeBlanc RL, Gearing RP, Bovee TD, Siegall CB, et al. (2003) Development of potent monoclonal antibody auristatin conjugates for cancer therapy. *Nat Biotechnol.* **21**:778-84.
- Gualberto A. (2012) Brentuximab Vedotin (SGN-35), an Antibody-Drug Conjugate for the Treatment of CD30-positive Malignancies. *Expert Opin Investig Drugs* **21**: 205-16.
- Gikanga B, Adeniji NS, Patapoff TW, Chih HW, Yi L. (2016) Cathepsin B Cleavage of vcMMAE-Based Antibody-Drug Conjugate Is Not Drug Location or Monoclonal Antibody Carrier Specific. *Bioconjug Chem* **27**:1040-9.

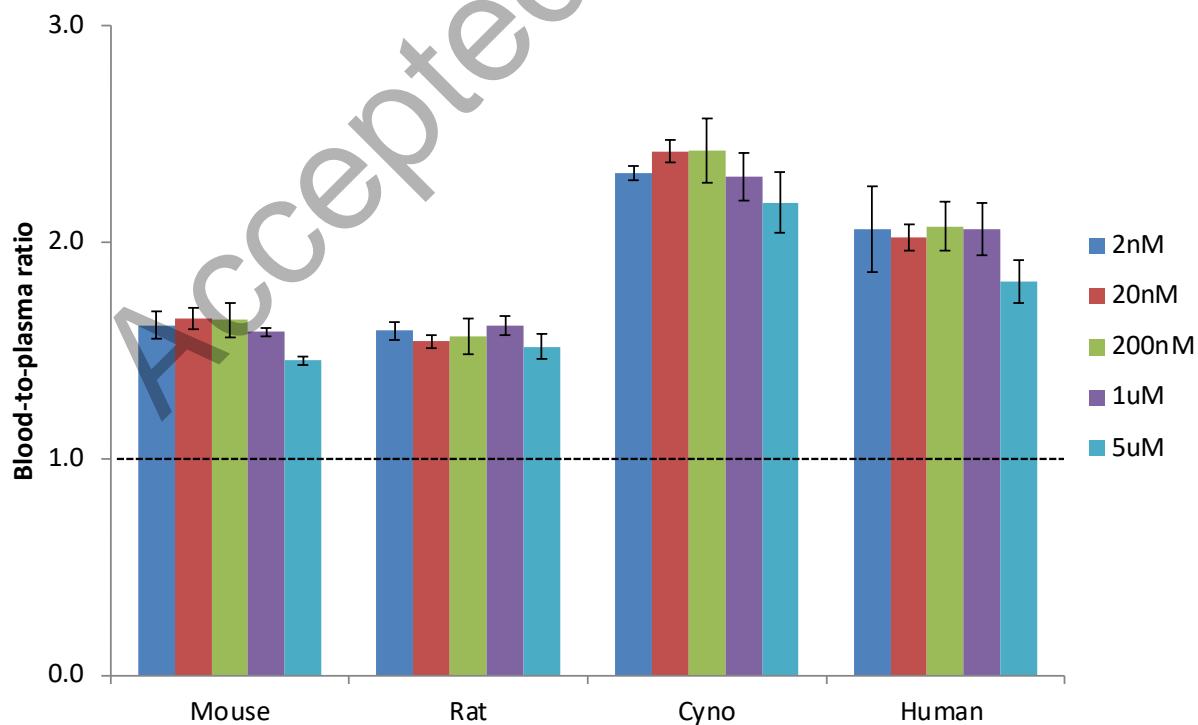
- Junutula JR, Raab H, Clark S, Bhakta S, Leipold DD, Weir S, Chen Y, Simpson M, Tsai SP, Dennis MS, et al. (2008) Site-specific conjugation of a cytotoxic drug to an antibody improves the therapeutic index. *Nat Biotechnol* **26**:925-932.
- Kwakye RA, Kuntworbe N, Ofori-Kwakye K, Osei YA. (2018) Detection, quantification, and investigation of the red blood cell partitioning of cryptolepine hydrochloride. *J Pharm Pharmacogn Res* **6**:260-270.
- Li C, Zhang C, Li Z, Samineni D, Lu D, Wang B, Chen SC, Zhang R, Agarwal P, Fine BM, et al. (2020) Clinical pharmacology of vc-MMAE antibody-drug conjugates in cancer patients: learning from eight first-in-human Phase 1 studies. *MAbs* **12**:1699768.
- Lu D, Jin JY, Girish S, Agarwal P, Li D, Prabhu S, Dere RC, Saad OM, Nazzal D, Koppada N, et al. (2015) Semi-mechanistic Multiple-Analyte Pharmacokinetic Model for an Antibody-Drug-Conjugate in Cynomolgus Monkeys. *Pharm Res* **32**:1907-19.
- Lu T, Gibiansky L, Li X, Li C, Shi R, Agarwal P, Hirata J, Miles D, Chanu P, Girish S, et al. (2020) Exposure-safety and exposure-efficacy analyses of polatuzumab vedotin in patients with relapsed or refractory diffuse large B-cell lymphoma. *Leuk Lymphoma*. **61**(12):2905-2914.
- Lucas AT, Price LSL, Schorzman AN, Storrie M, Piscitelli JA, Razo J, Zamboni WC. (2018) Factors Affecting the Pharmacology of Antibody-Drug Conjugates. *Antibodies (Basel)* **7**:10.
- Masters JC, Nickens DJ, Xuan D, Shazer RL, Amantea M. (2018) Clinical toxicity of antibody drug conjugates: a meta-analysis of payloads. *Invest New Drugs* **36**:121-135.

- Montel-Hagen A, Blanc L, Boyer-Clavel M, Jacquet C, Vidal M, Sitbon M, Taylor N. (2008) The Glut1 and Glut4 glucose transporters are differentially expressed during perinatal and postnatal erythropoiesis. *Blood* **112(12)**:4729-38
- Nair AB, Jacob S. A simple practice guide for dose conversion between animals and human. *J Basic Clin Pharma* 2016;**7**:27-31.
- Shen BQ, Bumbaca D, Saad O, Yue Q, Pastuskovas CV, Khojasteh SC, Tibbitts J, Kaur S, Wang B, Chu YW, et al. (2012) Catabolic fate and pharmacokinetic characterization of trastuzumab emtansine (T-DM1): an emphasis on preclinical and clinical catabolism. *Curr Drug Metab.* **13**:901-10.
- Yip V, Lee MV, Saad OM, Ma S, Khojasteh SC, Shen BQ. Preclinical Characterization of the Distribution, Catabolism, and Elimination of a Polatuzumab Vedotin-Piiq (POLIVY[®]) Antibody-Drug Conjugate in Sprague Dawley Rats. (2021) *J Clin Med.* **10(6)**:1323
- Yu S, Li S, Yang H, Lee F, Wu JT, Qian MG. (2005) A novel liquid chromatography/tandem mass spectrometry based depletion method for measuring red blood cell partitioning of pharmaceutical compounds in drug discovery. *Rapid Commun Mass Spectrom* **19**:250-4.
- Zhang S, Zhou D, Zheng C, Xiong P, Zhu W, Zheng D. (2021) Preclinical evaluation of a novel antibody-drug conjugate targeting DR5 for lymphoblastic leukemia therapy. *Mol Ther Oncolytics.* **21**:329-339

A. [³H]-MMAE



B. [³H]-Chloroquine



C. [³H]-Verapamil

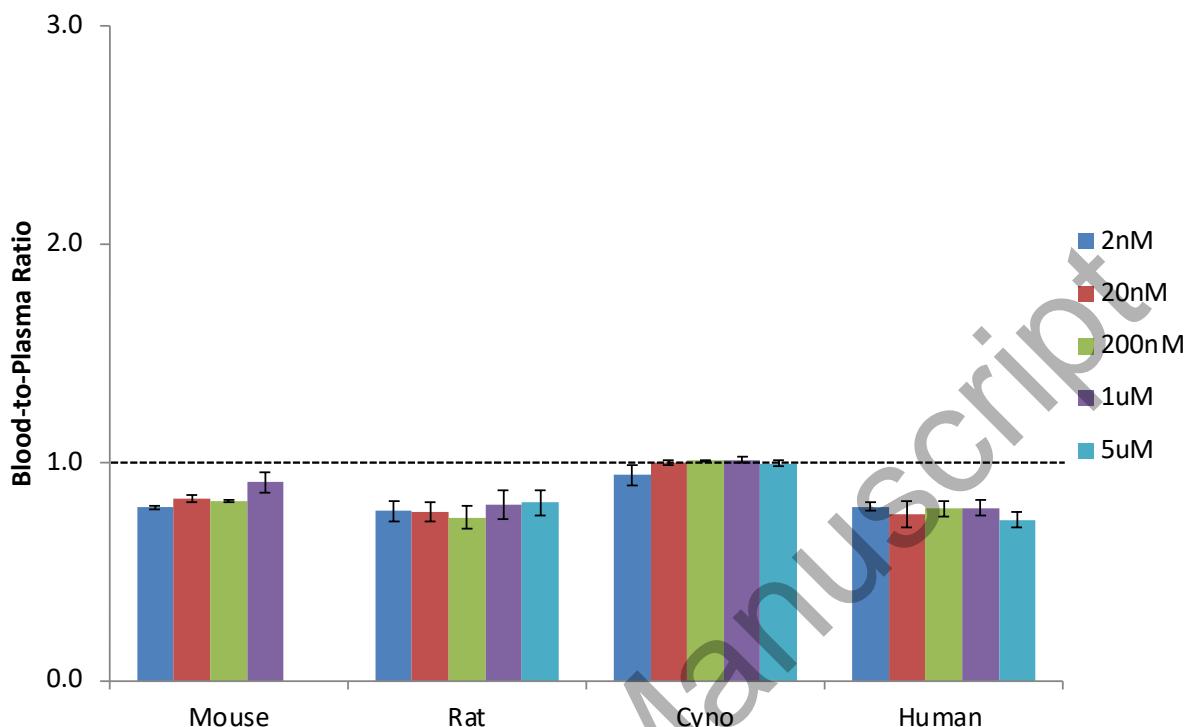


Figure 2. *In vitro* assessment of red-blood cell partitioning in human and animal blood. Molecule with blood-to-plasma ratio of greater than 1 is considered to be strongly associated with red-blood cell. **A)** [³H]-MMAE displayed a concentration- and species-dependent red blood cell partitioning as blood-to-plasma ratio varies with mouse blood at low concentration having the highest blood-to-plasma ratio and decreases with increase concentration. The blood-to-plasma ratio also decreased when rat blood was used instead of mouse blood and it further decreased with monkey and human blood. **B)** [³H]-Chloroquine is a positive control for this experiment and its blood-to-plasma ratio were all greater than 1 across different species and concentrations. **C)** [³H]-Verapamil is a negative control for this experiment and its blood-to-plasma ratio were all less than 1 across different species and concentrations. Dash-line at blood-to-plasma ratio at 1.

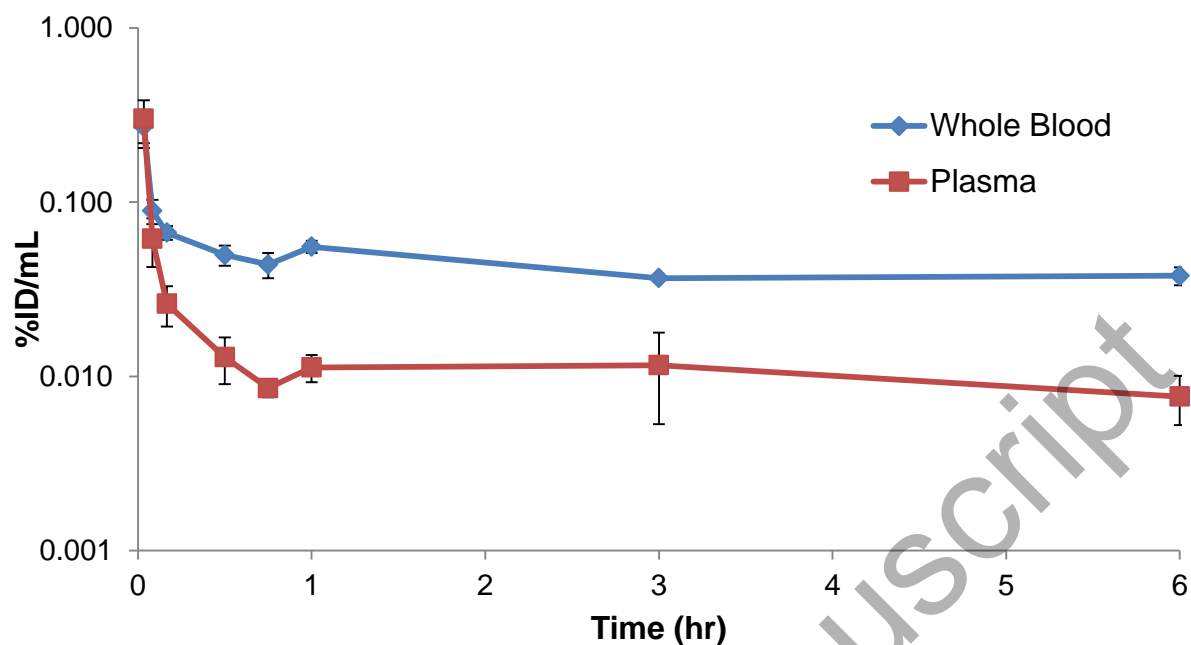


Figure 3. Systemic PK of unconjugated [^3H]-MMAE following single IV administration in rat. Radioactivity of [^3H]-MMAE (as % of injected dose per ml of volume) from whole blood and plasma in rats up to 6 hours post administration. Radioactivity concentration was fairly similar between blood and plasma initially, then increase to about 5-fold higher in blood compared to plasma, suggesting a strong partition to red blood cells.

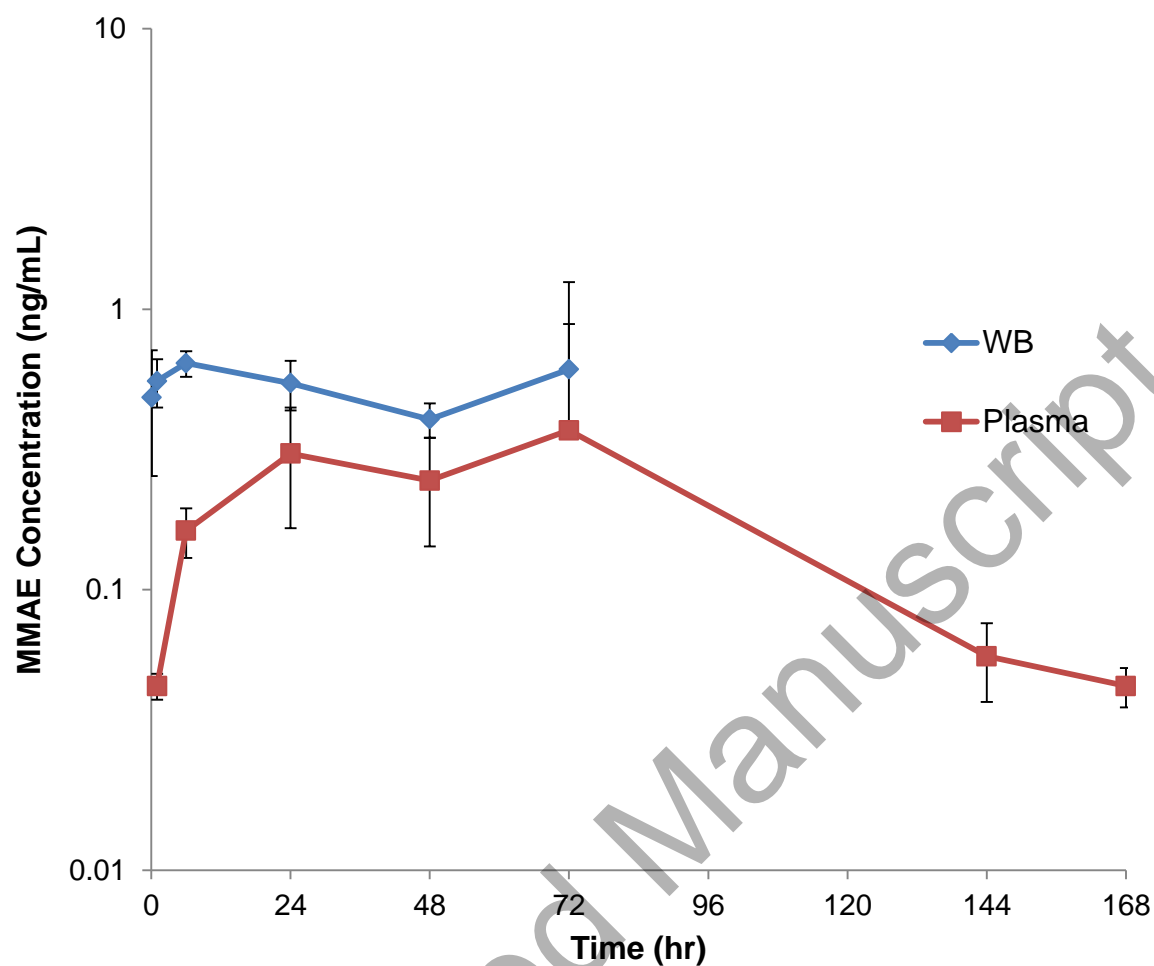


Figure 4. Plasma and whole blood of unconjugated MMAE concentration after a single intravenous dose of pinatuzumab vedotin at 5 mg/kg in rats. All plasma concentration were lower than the blood concentration of the same sample with a maximum blood-to-plasma ratio of 12.2 at 1-hour post-dose to a minimum of 1.65 at 72-hours post-dose. Blood $AUC_{(1h-72h)}$ compared to plasma $AUC_{(1h-72h)}$ showed a ratio of 1.99 over this quantifiable time range.

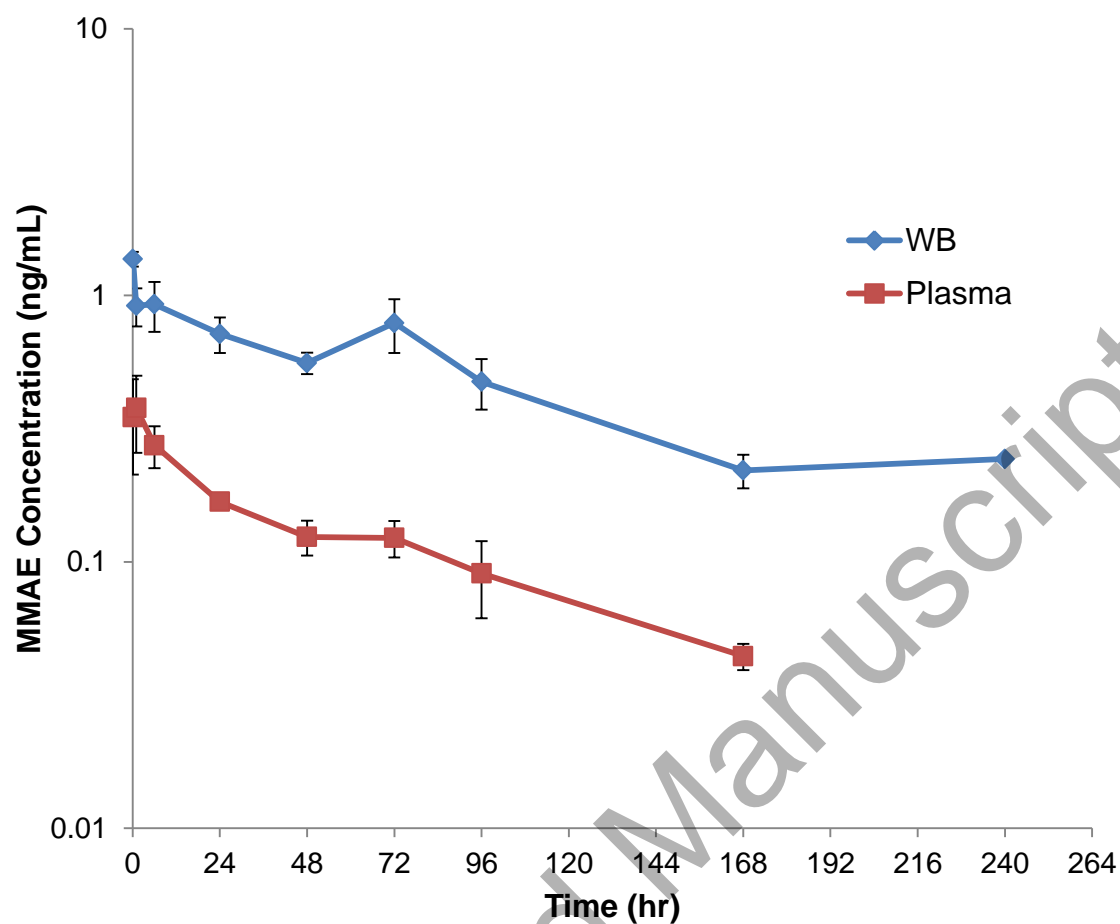


Figure 5. Plasma and whole blood of unconjugated MMAE concentration after a single intravenous dose of pinatuzumab vedotin at 5 mg/kg in mice. At 1-hour post-dose, deconjugated MMAE concentration in the blood was 2.41-fold of that of the plasma concentration. As both blood and plasma concentration decreased, the blood-to-plasma ratio increased to maximum of 6.40 at 72-hours post-dose. Overall, the Blood $AUC_{(1h-72h)}$ compared to plasma $AUC_{(1h-72h)}$ showed a ratio of 4.21.

Table 1. Maximum unconjugated MMAE concentration (C_{max}) detected in plasma from SCID mouse, Sprague Dawley rat, cynomolgus monkey (Lu et. al., 2015) and human (Li et al., 2020) after a single intravenous dose of 1) polatuzumab vedotin or 2) pinatuzumab vedotin. When C_{max} is normalized to dose (C_{max}/D), the human C_{max}/D is 37- to 98-fold higher than the pre-clinical species C_{max}/D .

Species	ADC Dose level (mg/kg)	Unconjugated MMAE C_{max} (ng/mL)	C_{max} normalized to dose (C_{max}/D)	Fold from human C_{max}/D
Human ¹	2.4	6.66	2.78	1
Cynomolgus Monkey ¹	3	0.085	0.0283	98
SD Rat ²	5	0.306	0.0612	45
SCID Mouse ²	5	0.378	0.0756	37

¹ Dosed with polatuzumab vedotin ² Dosed with pinatuzumab vedotin

Table 2. Average MMAE concentration (%ID/mL) in blood and plasma after a single dose of [³H]-MMAE at 200 μ g/kg in SD rat. Blood-to plasma ratio reached a maximum level of 5.13 at 0.75 hour post dose.

Time (hr)	Average blood concentration (%ID/mL)	Average plasma concentration (%ID/mL)	Blood-to-plasma ratio
0.0333	0.301	0.272	0.903
0.0833	0.0616	0.0890	1.44
0.1667	0.0261	0.0668	2.56
0.5	0.0129	0.0497	3.86
0.75	0.0086	0.0439	5.13
1	0.0113	0.0555	4.93
3	0.0116	0.0366	3.16
6	0.0077	0.0378	4.93

Table 3. Average unconjugated MMAE concentration (ng/mL) in blood and plasma after a single dose of pinatuzumab vedotin at 5 mg/kg in SD rat. Blood-to plasma ratio reached a maximum level of 12.2 at 1 hour post dose and leveled off at 1.65 by 72 hours post dose.

Time (hr)	Average blood concentration (ng/mL)	Average plasma concentration (ng/mL)	Blood-to-plasma ratio
0.0833	0.48	LLOQ (<0.0359)	N/A
1	0.555	0.045	12.2
6	0.642	0.162	3.95
24	0.545	0.306	1.78
48	0.405	0.245	1.65
72	0.610	0.370	1.65
96	LLOQ (<0.180)	0.058	N/A
168	LLOQ (<0.180)	0.045	N/A

Table 4. Average unconjugated MMAE concentration (ng/mL) in blood and plasma after a single dose of pinatuzumab vedotin at 5 mg/kg in SCID mouse. Blood-to plasma ratio reached a maximum level of 6.40 at 72 hours post dose and leveled off at around 5.

Time (hr)	Average blood concentration (ng/mL)	Average plasma concentration (ng/mL)	Blood-to-plasma ratio
0.0833	1.37	0.349	3.93
1	0.914	0.378	2.42
6	0.925	0.274	3.38
24	0.716	0.168	4.26
48	0.558	0.124	4.50
72	0.788	0.123	6.40
96	0.474	0.091	5.24
168	0.220	0.044	4.98